Aqueous Fibronectin Correlates With Severity of Macular Edema and Visual Acuity in Patients With Branch Retinal Vein Occlusion: A Proteome Study

Lasse Jørgensen Cehofski,[1–3] Kentaro Kojima,[4] Nobuhiro Terao,[4] Koji Kitazawa,[4] Sasikala Thineshkumar,[1] Jakob Grauslund,[1,3] Henrik Vorum,[5,6] and Bent Honoré[6,7]

[1]Department of Ophthalmology, Odense University Hospital, Odense, Denmark
[2]Department of Ophthalmology, Lillebaelt Hospital, Vejle, Denmark
[3]Department of Clinical Research, University of Southern Denmark, Odense, Denmark
[4]Department of Ophthalmology, Kyoto Prefectural University of Medicine, Kyoto, Japan
[5]Department of Ophthalmology, Aalborg University Hospital, Aalborg, Denmark
[6]Department of Clinical Medicine, Aalborg University, Aalborg, Denmark
[7]Department of Biomedicine, Aarhus University, Aarhus, Denmark

Correspondence: Lasse Jørgensen Cehofski, Department of Ophthalmology, Odense University Hospital, Sdr. Boulevard 29, 5000 Odense C, Denmark; lassecehofski@hotmail.com.

Received: April 8, 2020
Accepted: October 5, 2020
Published: December 3, 2020

Citation: Cehofski LJ, Kojima K, Terao N, et al. Aqueous fibronectin correlates with severity of macular edema and visual acuity in patients with branch retinal vein occlusion: A proteome study. *Invest Ophthalmol Vis Sci.* 2020;61(14):6. https://doi.org/10.1167/iovs.61.14.6

Purpose. Large-scale protein analysis may bring important insights into molecular changes following branch retinal vein occlusion (BRVO). Using proteomic techniques this study compared aqueous humor samples from patients with BRVO to age-matched controls.

Methods. Aqueous humor samples from treatment naive patients with BRVO complicated by macular edema ($n = 19$) and age-matched controls ($n = 18$) were analyzed with label-free quantification nano liquid chromatography – tandem mass spectrometry (LFQ nLC-MS/MS). The severity of macular edema was measured as central retinal thickness (CRT) with optical coherence tomography. Control samples were obtained prior to cataract surgery. Proteins were filtered by requiring quantification in at least 50% of the samples in each group without imputation of missing values. Significantly changed proteins were identified with a permutation-based calculation with a false discovery rate at 0.05.

Results. In BRVO, 52 proteins were differentially expressed. Regulated proteins were involved in cell adhesion, coagulation, and acute-phase response. Apolipoprotein C-III, complement C3, complement C5, complement factor H, fibronectin, and fibrinogen chains were increased in BRVO and correlated with CRT. Fibronectin also correlated with best corrected visual acuity (BCVA) and vascular endothelial growth factor (VEGF). Monocyte differentiation antigen CD14 (CD14) and lipopolysaccharide-binding protein (LBP) were upregulated in BRVO. Contactin-1 and alpha-enolase were downregulated in BRVO and correlated negatively with CRT.

Conclusions. Multiple proteins, including complement factors, fibrinogen chains, and apolipoprotein C-III, correlated with CRT, indicating a multifactorial response. Fibronectin correlated with BCVA, CRT, and VEGF. Fibronectin may reflect the severity of BRVO. The proinflammatory proteins CD14 and LBP were upregulated in BRVO.

Keywords: retina, branch retinal vein occlusion, proteomics, mass spectrometry, macular edema

Branch retinal vein occlusion (BRVO) is the most frequent retinal vascular disease after diabetic retinopathy.[1] Macular edema is the most common cause of visual impairment in BRVO.[1] Important elements in the development of macular edema secondary to BRVO include vascular endothelial growth factor (VEGF), VEGF receptor-1 and 2, as well as an inflammatory response mediated by interleukin-6, interleukin-8, monocyte chemoattractant protein 1, and platelet-derived growth factor.[2–10] Although this subset of proteins is well-characterized in BRVO, there is very limited knowledge about large-scale intraocular protein changes in samples from humans with BRVO.[11]

Large-scale protein analyses are effectively performed with mass spectrometry-based proteomic techniques, which aim at identifying and quantifying the entire set of proteins in a given tissue or body fluid.[12–16] Proteome studies of aqueous humor may bring valuable insights into molecular changes following BRVO.[11,17] However, the human aqueous proteome of BRVO remains largely unstudied with mass spectrometry except for a study on aqueous humor from six BRVO patients, which was published by Yao et al.[18] in 2013. With major advances in recent years, proteomic techniques allow for in-depth protein analysis that may elucidate molecular mechanisms underlying ocular diseases.[11–17] In

Table 1. Samples for Proteomic Analysis

	BRVO Group	Control Group	*P* Value
Number of samples (*n*)	19	18	
Age (years)	70.9 ± 7.8*	72.1 ± 13.6*	0.76
Sex (M/F)	10/9	8/10	
Size of macular edema (μm)	519 ± 257*	–	–
BCVA (logMAR)	0.53 ± 0.39*	–	–
Patients with retinal area of nonperfusion ≤ 5 disc areas (*n*)	5	–	–
Patients with retinal area of nonperfusion > 5 disc areas (*n*)	14	–	–

* Data are expressed as mean ± standard deviation.

the present study, we used advanced proteomic techniques to compare 19 aqueous humor samples from patients with BRVO and macular edema with 18 age-matched controls.

Methods

Samples

The study was conducted in compliance with the institutional review board of Kyoto Prefectural University of Medicine from which approval for the study was obtained (permission RBMR-C-864-6). The study adhered to the tenets of the Declaration of Helsinki. Aqueous humor samples from treatment naive patients with BRVO complicated by macular edema ($n = 19$) and age-matched controls ($n = 18$) were donated from the biobank of Kyoto Prefectural University Hospital, Kyoto, Japan, for proteomic analysis (Table 1). Informed consent to use samples from the biobank was obtained from all patients after explanation of the nature and possible consequences of the study. Statistical analysis by the Student's *t*-test was used to verify that there was no statistically significant difference in age between the BRVO group and the age-matched control group (Table 1). All patients in the BRVO group had BRVO complicated by macular edema and were treatment naive. Duration of macular edema less than 3 months was required. In the BRVO group, exclusion criteria were glaucoma including neovascular glaucoma, iris rubeosis, hyphema, retinal neovascularization, vitreous hemorrhage, previous retinal photocoagulation, and diabetes mellitus. Patients with BRVO who used any kind of eye drops 3 months prior to sample collection were also excluded. Control samples were from age-matched patients from whom aqueous humor samples were obtained prior to cataract surgery. Patients in the control group had no other disease than cataract. Best corrected visual acuity (BCVA) was measured as the logarithm of the minimum angle of resolution (logMAR). Swept Source OCT (DRI-OCT Triton; Topcon, Tokyo, Japan) was used for optical coherence tomography (OCT) examination. The severity of macular edema was measured as central retinal thickness (CRT) with the caliper tool of the Topcon OCT software. Fluorescein angiography was performed with confocal scanning laser ophthalmoscope (Heidelberg Retina Angiograph 2; Heidelberg Engineering, Heidelberg, Germany), and the area of retinal nonperfusion was measured in disc areas using the "draw lesion" tool in Heidelberg Retinal Angiography 2.

For confirmation of key findings of the proteomic analysis, additional BRVO samples ($n = 15$) and control samples ($n = 5$) were acquired from the biobank for enzyme-linked immunosorbent assay (ELISA) (Table 2). Eight samples from the BRVO group were also used for proteomic analysis. BRVO samples and control samples were age-matched and selected according to the inclusion and exclusion criteria stated earlier. Statistical analysis by the Student's *t*-test was used to verify that there was no statistically significant difference in age between the BRVO group and the age-matched control group (Table 2).

Table 2. Samples for Validation of Proteomic Analysis by ELISA

	BRVO Group	Control Group	*P* Value
Number of samples (*n*)	15*	5	
Age (years)	70.6 ± 11.6†	75.6 ± 6.3†	0.38
Sex (M/F)	8/7	2/3	
Size of macular edema (μm)	542 ± 226†	–	–
BCVA (logMAR)	0.59 ± 0.40†	–	–

* Samples from eight patients with BRVO were also used for proteomic analysis.
† Data are expressed as mean ± standard deviation.

Sample Preparation for Mass Spectrometry

Samples were stored at −80°C until preparation was initiated. Protein concentrations were measured with an infrared spectrometer (Direct Detect, Darmstadt, Germany). Samples were prepared according to the S-Trap Micro spin column digestion protocol from ProtiFi (Huntington, NY, USA). The volume of each sample was measured, and an equal volume of 2 × SDS lysis buffer (10% SDS, 100 mM triethylammonium bicarbonate [TEAB], pH 7.55) was added. The samples were centrifuged at 13.000*g* for 8 minutes. Disulfide bonds were reduced by adding tris(2-carboxyethyl)phosphine hydrochloride (TCEP) to the protein solution in SDS to a final concentration of 10 mM, followed by heating for 10 minutes at 95°C. The protein solution was cooled to room temperature. Cysteines were alkylated by adding iodoacetamide to a final concentration of 40 mM. To the SDS lysate, 12% aqueous phosphoric acid at 1:10 was added to a final concentration of 1.2% phosphoric acid. S-Trap buffer (90% methanol, 100 mM TEAB) was added. The buffer mixture was transferred into a microcolumn followed by centrifugation at 4000*g* until the buffer had passed through the S-Trap column. S-Trap binding buffer was added, followed by centrifugation at 4000*g*. Washing with the S-Trap binding buffer was performed three times. The S-Trap microcolumn was moved to a new 1.7 mL sample tube for digestion. A total of 20 μL digestion buffer was added into the top of the microcolumn. The column was incubated overnight at 37°C.

Peptides were eluted first with 40 μL of 50 mM TEAB and then with 0.2% formic acid. Elutions were centrifuged at 4000*g*. Hydrophobic peptides were recovered with an elution of 35 μL 50% acetonitrile containing 0.2% formic acid. Elutions were pooled. The peptide concentration was measured with a fluorescence-based technique with tryptophan used as a standard with an excitation at 295 nm and

Investigative Ophthalmology & Visual Science

emission at 350 nm as previously described.[19] Each sample was dried in a vacuum centrifuge and stored at −80°C.

Quantitative Mass Spectrometry by Label-Free Quantification Nano Liquid Chromatography – Tandem Mass Spectrometry (LFQ nLC-MS/MS)

Samples were resuspended in 0.1% formic acid and analyzed with LFQ nLC-MS/MS. Of each sample, 0.7 to 1.0 µg was analyzed in triplicates. Mass spectrometry was performed on an Orbitrap Fusion Tribrid mass spectrometer (Thermo Fisher Scientific Instruments, Waltham, MA, USA) coupled to a Dionex UltiMate 3000 RSLC nano system (Thermo Fisher Scientific Instruments, Waltham, MA, USA). The mass spectrometer was equipped with an EasySpray ion source (Thermo Fisher Scientific Instruments). Liquid chromatography and label-free quantification (LFQ) were performed as described in a recent article[20] with few modifications. The orbitrap scan range (m/z) was 375 to 1500. The elution gradient was 3h, established by mixing buffer A (99.9% water and 0.1% formic acid) and buffer B (99.9% acetonitrile and 1% formic acid). Using the MaxQuant software version 1.6.6.0 (Max Planck Institute of Biochemistry, Martinsried, Germany; https://maxquant.net/maxquant/) for LFQ analysis,[21] raw data files were searched against the UniProt *Homo sapiens* database (www.uniprot.org) downloaded on August 10, 2019. Settings for the database search were published in a previous work.[20] Unfiltered results of the database search are available in Supplementary File S1.

Mass spectrometry data were further processed with Perseus software version 1.6.2.3 (Max Planck Institute of Biochemistry, Martinsried, Germany; https://maxquant.net/perseus/) to remove poorly identified proteins as described in a previous article.[22] LFQ values were $\log_2$ transformed, and mean LFQ values were calculated. At least two unique peptides were required for successful protein identification. Proteins were required to be successfully identified and quantified in at least 50% of the samples in each group. The median technical coefficient of variation was calculated for each of the proteins in each sample. The mean value for the samples was 11.3% (range, 6.49%–16.1%).

Statistics

Statistical analysis was performed on proteins that were successfully identified and quantified in at least 50% of the samples in the BRVO group and 50% of the samples in the control group. No imputation of missing values was performed prior to statistical analysis. Statistical analysis by the Student's *t*-test was conducted in Perseus to compare BRVO with controls. Furthermore, a subgroup analysis was performed to compare BRVO with greater than 5 disc areas of retinal nonperfusion and BRVO with less than or equal to 5 disc areas of retinal nonperfusion. Correction for multiple hypothesis testing was performed using the permutation-based method[23] in Perseus with the number of randomizations set to 250 and an S_0 parameter of 0.1. The false discovery rate was set to 0.05. CRT values were $\log_{10}$ transformed prior to calculation of correlations to make the CRT values normally distributed. Correlations were calculated in STATA 16.0 (StataCorp, College Station, TX, USA) using Pearson's correlation coefficient (r). Correlations were considered statistically significant if $P < 0.05$. Two-way scatter plots with prediction from a linear regression were created with STATA 16.0.

Bioinformatic analysis of statistically significantly changed proteins was performed with GeneCodis software[24–26] (https://genecodis.genyo.es/) as previously described.[27] Cluster analysis of statistically significantly regulated proteins was performed with STRING 11.0 (string-db.org).[28–30] If more than one protein was listed in the IDs, the first listed UniProt ID was used for STRING analysis. If an isoform was not recognized by STRING, the regular UniProt ID without isoform was used. Cluster analysis was performed with the Markov Cluster Algorithm set to 2.

Enzyme-Linked Immunosorbent Assay (ELISA)

Enzyme-Linked Immunosorbent Assay (ELISA) was performed to measure aqueous concentrations of fibronectin and VEGF in 15 BRVO samples and 5 controls (Table 2). ELISA was conducted with the ab219046 Human Fibronectin SimpleStep ELISA kit (Abcam, UK)[31,32] and the ab222510 Human VEGF SimpleStep ELISA Kit (Abcam, UK).[33] Samples for fibronectin quantification were diluted 1:250, and samples for VEGF quantification were diluted 1:2. Assay preparation was performed according to the manufacturer's instructions. A volume of 50 µL of standard or sample was added to the wells following addition of 50 µL antibody solution (1:10 capture antibody solution and 1:10 detector antibody in Antibody Diluent 4BR from the kit). The solutions were incubated for 1 hour at room temperature on a plate shaker set to 480 rpm. Each well was washed with 3 × 350 µL wash buffer (1:10 Wash Buffer PT 10X from ELISA kit, Abcam, UK, in deionized water). A volume of 100 µL of TMB Development Solution (Abcam, UK) was added to each well followed by incubation for 10 minutes in the dark on a plate shaker set to 480 rpm. A volume of 100 µL of Stop Solution (provided in kit) was added to each well and the plate was shaken on a plate shaker for 1 minute. The optical density was recorded at 450 nm. The Student's *t*-test and Pearson's correlation coefficient (r) were used for statistical analysis of the ELISA data. Differences and correlations were considered statistically significant if $P < 0.05$. Two-way scatter plots based on ELISA data with prediction from a linear regression were created in STATA 16.0.

Results

A total of 1403 proteins were successfully identified in the combined set of aqueous samples (Supplementary File S2). A total of 242 aqueous humor proteins were successfully identified and quantified in at least 50% of the samples in each group (Supplementary File S3) and statistical analysis was performed on these proteins.

After correction for multiple hypothesis testing, a total of 52 proteins were statistically significantly changed in content in BRVO compared with controls (Table 3, Fig. 1A). Among the 52 proteins that were changed in content, 26 proteins were increased in content following BRVO, whereas another 26 proteins were decreased in content in BRVO (Table 3).

Proteins that were changed in expression level in BRVO compared with controls were involved in cell adhesion, blood coagulation, platelet activation, and platelet degranulation (Fig. 2). BRVO was also associated with response to lipopolysaccharide, chemotaxis, and

Investigative Ophthalmology & Visual Science

Table 3. Statistically Significantly Regulated Proteins in BRVO Versus Controls

Protein ID	Protein Name	Gene Name	*P* Value	Fold Change BRVO/Control
P02675	Fibrinogen beta chain	FGB	1.92×10^{-9}	17.32
P02679	Fibrinogen gamma chain	FGG	1.16×10^{-8}	6.89
P02671	Fibrinogen alpha chain	FGA	1.72×10^{-7}	5.25
P02751-3	Fibronectin	FN1	1.10×10^{-6}	2.80
P02656	Apolipoprotein C-III	APOC3	0.00095	2.47
P01031	Complement C5	C5	6.92×10^{-5}	1.75
P01861	Ig gamma-4 chain C region	IGHG4	0.031	1.74
P08603	Complement factor H	CFH	2.51×10^{-6}	1.73
P04004	Vitronectin	VTN	0.00074	1.72
P24592	Insulin-like growth factor-binding protein 6	IGFBP6	0.016	1.67
P02749	Beta-2-glycoprotein 1	APOH	3.14×10^{-5}	1.67
P02746	Complement C1q subcomponent subunit B	C1QB	0.0081	1.61
P02753	Retinol-binding protein 4	RBP4	0.0018	1.60
P06727	Apolipoprotein A-IV	APOA4	0.0067	1.55
P36222	Chitinase-3-like protein 1	CHI3L1	0.0071	1.54
P19827	Inter-alpha-trypsin inhibitor heavy chain H1	ITIH1	0.012	1.53
P05546	Heparin cofactor 2	SERPIND1	0.00043	1.50
P08571	Monocyte differentiation antigen CD14	CD14	3.23×10^{-5}	1.49
P05090	Apolipoprotein D	APOD	0.0036	1.49
P18428	Lipopolysaccharide-binding protein	LBP	0.0022	1.48
Q14520	Hyaluronan-binding protein 2 chain	HABP2	0.0010	1.44
P00734	Prothrombin	F2	0.00030	1.42
P01042	Kininogen-1	KNG1	0.0031	1.40
Q14624	Inter-alpha-trypsin inhibitor heavy chain H4	ITIH4	0.0059	1.39
P01024	Complement C3	C3	0.0010	1.38
P01023	Alpha-2-macroglobulin	A2M	0.00079	1.37
Q8IZJ3-2	C3 and PZP-like alpha-2-macroglobulin domain-containing protein 8	CPAMD8	0.0023	0.78
P13473	Lysosome-associated membrane glycoprotein 2	LAMP2	0.0037	0.72
P07711	Cathepsin L1	CTSL	0.0020	0.71
Q86UX2	Inter-alpha-trypsin inhibitor heavy chain H5	ITIH5	0.0052	0.70
Q12860	Contactin-1	CNTN1	0.0011	0.68
Q08629	Testican-1	SPOCK1	0.0070	0.67
O75326	Semaphorin-7A	SEMA7A	0.018	0.67
Q14515-2	SPARC-like protein 1	SPARCL1	0.010	0.67
P13591	Neural cell adhesion molecule 1	NCAM1	0.0030	0.66
P35555	Fibrillin-1	FBN1	0.020	0.65
Q13822	Ectonucleotide pyrophosphatase/phosphodiesterase family member 2	ENPP2	0.00015	0.65
Q02413	Desmoglein-1	DSG1	0.013	0.65
P98164	Low-density lipoprotein receptor-related protein 2	LRP2	0.00020	0.64
O94985-2	Calsyntenin-1	CLSTN1	0.0013	0.63
P78509-3	Reelin	RELN	0.016	0.61
Q99574	Neuroserpin	SERPINI1	0.0027	0.61
Q08380	Galectin-3-binding protein	LGALS3BP	0.00029	0.58
P98160	Basement membrane-specific heparan sulfate proteoglycan core protein	HSPG2	0.011	0.57
P06733	Alpha-enolase	ENO1	0.028	0.55
Q06481	Amyloid-like protein 2	APLP2	4.32×10^{-5}	0.49
Q01469	Fatty acid-binding protein, epidermal	FABP5	0.013	0.45
P55083	Microfibril-associated glycoprotein 4	MFAP4	0.00028	0.44
P22914	Beta-crystallin S	CRYGS	0.00036	0.37
P31151	Protein S100-A7	S100A7	0.033	0.34
P06702	Protein S100-A9	S100A9	0.015	0.31
P05109	Protein S100-A8	S100A8	0.030	0.30

acute-phase response (Fig. 2). Proteins with cell adhesion features included fibronectin, hyaluronan-binding protein 2 chain, testican-1, microfibrillar-associated protein 4, neural cell adhesion molecule 1, contactin-1, calsyntenin-1, galectin-3-binding protein, and reelin. Proteins involved in response to lipopolysaccharide included S100A7, S100A8, S100A9, lipopolysaccharide-binding protein (LBP), and monocyte differentiation antigen CD14 (CD14). Proteins with chemotactic features included complement C5, S100A8, S100A9, ectonucleotide pyrophosphatase, and heparin cofactor 2. LBP, fibronectin, prothrombin, and inter-alpha-trypsin inhibitor heavy chain H4 were identified as acute-phase response proteins.

STRING cluster analysis revealed a major cluster of proteins consisting of fibronectin, fibrinogen chains, complement factors, and apolipoproteins (Fig. 3). Another cluster consisted of S100A7, S100A8, S100A9, CD14, LBP, and complement C1q subcomponent subunit B (Fig. 3).

Investigative Ophthalmology & Visual Science

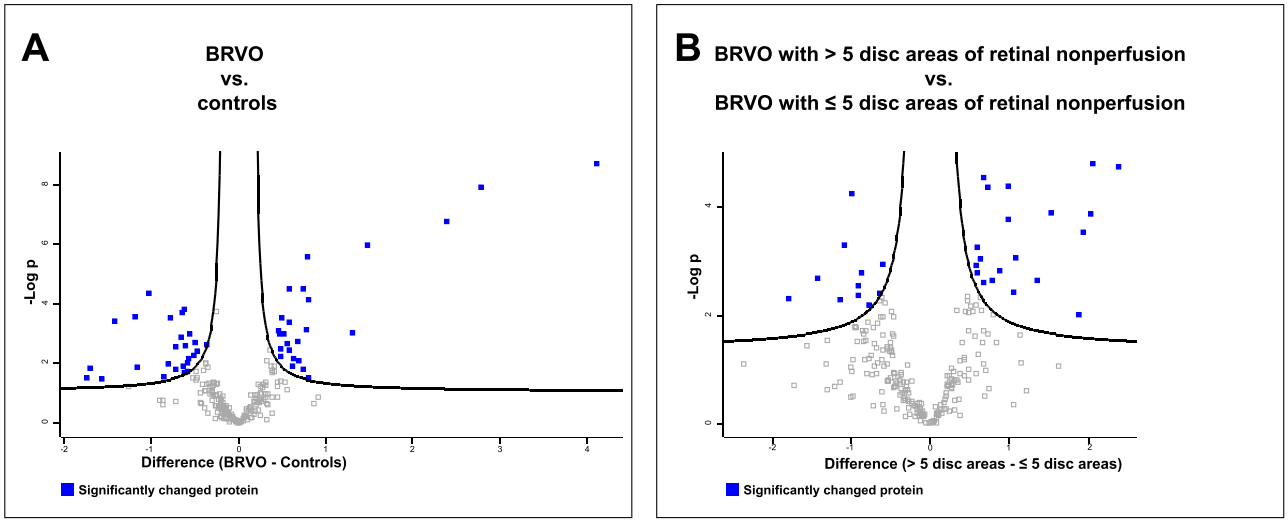

Figure 1. Volcano plots. (**A**) Log_2 transformed abundance ratios for each protein are plotted on the *x*-axis. Negative log_{10} transformed *P* values are plotted on the *y*-axis. A false discovery rate of 0.05 was applied. Statistically significantly changed proteins are localized above the full curves. (**A**) BRVO versus age-matched control samples. A total of 52 statistically significantly changed proteins (*blue squares*) were identified. (**B**) BRVO with greater than 5 disc areas of retinal nonperfusion versus BRVO with less than or equal to 5 disc areas of retinal nonperfusion. A total of 31 significantly changed proteins (*blue squares*) were identified.

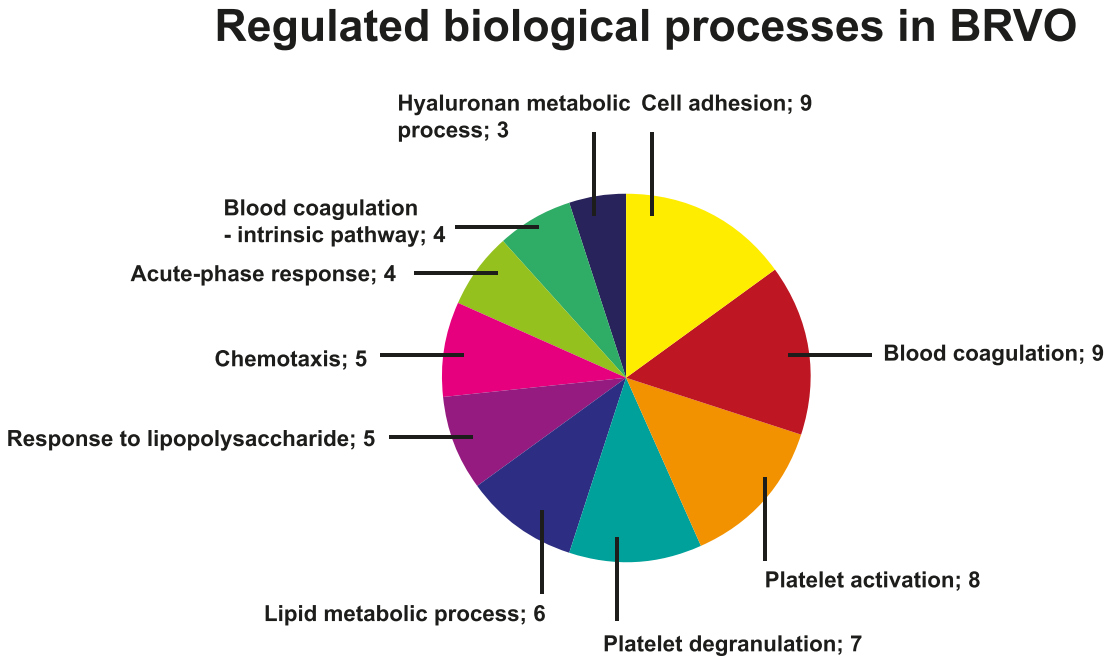

Figure 2. Regulated biological processes in BRVO compared with controls. Numbers refer to the number of proteins that represent a given biological process.

Furthermore, a cluster of reelin, neural cell adhesion molecule 1, and contactin-1 was identified.

Eleven proteins were positively correlated to severity of macular edema, whereas two proteins were negatively correlated to severity of macular edema (Table 4, Figs. 4, 5). Proteins that were positively correlated to CRT included apolipoprotein C-III; complement C3; complement C5; complement factor H; fibrinogen chains α, β, and γ; fibronectin; heparin cofactor 2; as well as inter-alpha-trypsin inhibitor chain H1; and chain H4 (Table 4, Figs. 4, 5). Alpha-enolase and contactin-1 were negatively correlated to CRT (Table 4, Figs. 4K, 4L).

Proteomic analysis revealed an increased level of fibronectin in BRVO compared with controls (fold change = 2.80, $P = 0.0000011$) (Table 3; Fig. 5A). ELISA confirmed that fibronectin was significantly elevated in BRVO (0.10 µg/mL) compared with control subjects (0.022 µg/mL) ($P = 0.011$) (Fig. 5B). Proteomic analysis identified a correlation between aqueous fibronectin and BCVA ($r = 0.46$; $P = 0.049$) (Fig. 5C) (Supplementary File S4). The correlation between

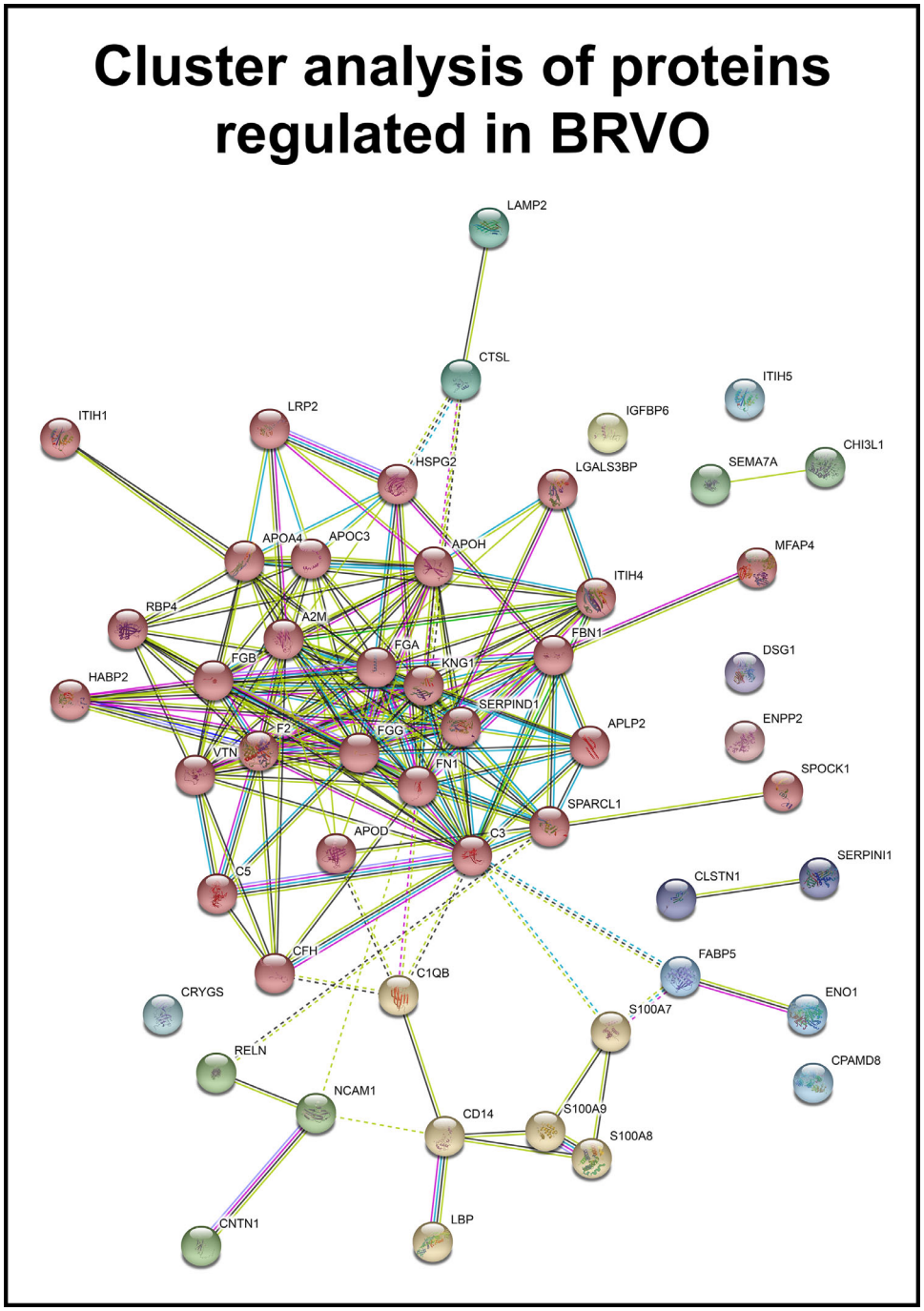

Figure 3. STRING cluster analysis of regulated proteins in BRVO compared with controls. A major cluster (*red nodes*) was formed by fibrinogen chains (FGA, FGB, FGG), fibronectin (FN1), apolipoproteins (APOA4, APOC3, APOD), and complement factors (C3, C5, CFH). Another cluster (*yellow nodes*) was formed by complement C1q subcomponent subunit B (C1QB), monocyte differentiation antigen CD14 (CD14), lipopolysaccharide binding protein (LBP), S100A7, S100A8, and S100A9.

fibronectin and BCVA was confirmed with ELISA (r = 0.56; P = 0.032) (Fig. 5D). Proteome analysis identified a statistically significant correlation between fibronectin and the severity of macular edema measured as CRT (r = 0.60; P = 0.0061) (Table 4; Fig. 5E). This correlation was confirmed with ELISA (r = 0.53; P = 0.042) (Fig. 5F). Aqueous fibronectin correlated with VEGF in the BRVO samples (r = 0.70; P = 0.0039) (Fig. 6) (Supplementary File S5).

Subgroup analysis revealed that the aqueous fibronectin content was higher in BRVO with greater than 5 disc areas of retinal nonperfusion compared with BRVO with less than or equal to 5 disc areas of retinal nonperfusion (fold change = 2.88; P = 0.00013) (Fig. 1B, Table 5). A total of 31 proteins were significantly different in BRVO with greater than 5 disc areas of nonperfusion compared with BRVO with less than or equal to 5 disc areas of nonperfusion (Fig. 1B, Table 5). Patients with BRVO and greater than 5 disc areas of

Table 4. Correlations Between Proteomic Data and Severity of Macular Edema

Protein ID	Protein Name	Correlation, *r*	*P* Value
P02671	Fibrinogen alpha chain	0.68	0.0013
P02679	Fibrinogen gamma chain	0.67	0.0018
P02675	Fibrinogen beta chain	0.64	0.0029
P02751-3	Fibronectin	0.60	0.0061
P02656	Apolipoprotein C-III	0.54	0.018
Q14624	Inter-alpha-trypsin inhibitor heavy chain H4	0.54	0.018
P19827	Inter-alpha-trypsin inhibitor heavy chain H1	0.52	0.022
P08603	Complement factor H	0.51	0.027
P01024	Complement C3	0.47	0.041
P01031	Complement C5	0.47	0.044
P05546	Heparin cofactor 2	0.46	0.049
Q12860	Contactin-1	−0.50	0.029
P06733	Alpha-enolase	−0.52	0.023

retinal nonperfusion had higher aqueous levels of fibrinogen chains, apolipoprotein C-III, and apolipoprotein A-IV, and lower aqueous levels of amyloid-like protein 2, contactin-1, reelin, and alpha-enolase (Table 5).

Discussion

The presented study aimed at identifying large-scale protein changes in aqueous humor from patients with BRVO giving insights into intraocular molecular changes of the condition. A multitude of proteins were regulated in BRVO compared with age-matched controls. Protein changes were generally more pronounced in BRVO with greater than 5 disc areas of retinal nonperfusion. Multiple proteins were correlated to severity of macular edema indicating a multifactorial nature of the condition.

Fibronectin correlated with BCVA and severity of macular edema. Fibronectin is a 230 to 270 kDa glycoprotein that exists in a soluble form and an insoluble form.[34–36] The soluble form in the aqueous humor regulates thrombosis and accelerates wound healing.[35,36] At the wall of injured vessels the soluble form of fibronectin is rapidly deposited and promotes platelet aggregation when linked with fibrin.[37] Our data indicated that the increased level of fibronectin was associated with retinal ischemia as the content of fibronectin was higher in BRVO with greater than 5 disc areas of retinal nonperfusion. The correlation between fibronectin and BCVA may be explained by the fact that fibronectin was associated with severity of macular edema and retinal nonperfusion, which are complications that cause visual impairment in BRVO. A strong correlation between fibronectin and VEGF was observed in BRVO. The increased level of fibronectin in BRVO may reflect a stage of increased VEGF-driven vascular permeability with leakage of fibronectin. In summary, aqueous fibronectin may be an indicator of the severity of BRVO.

The plasma proteins, such as fibrinogen chains, apolipoproteins, and complement factors, were upregulated in BRVO and correlated with severity of macular edema. The upregulation of the mentioned plasma proteins may represent an activation of the coagulation cascade, as well as a disruption of the blood-retinal barrier that results in leakage of plasma proteins.[11,17] Patients with BRVO and greater than 5 disc areas of retinal nonperfusion had higher levels of fibrinogen chains, apolipoproteins, and complement factors, which may be explained by increased vascular permeability due to ischemia.[9,10,38,39] BRVO was associated with regulation of proteins involved in "response to lipopolysaccharide," including the proinflammatory proteins LBP, CD14, S100A7, S100A8, and S100A9 (Fig. 2). Lipopolysaccharide is the major component of the outer membrane of gram-negative bacteria. Recognition of lipopolysaccharide requires LBP, CD14, and Toll-like receptor 4 (TLR4) that have regulatory functions in the innate immune system.[40,41] LBP and CD14 may contribute to the inflammatory response in BRVO, but did not correlate with severity of macular edema and BCVA.

S100A7, S100A8, and S100A9 belong to the S100 protein family of small calcium-binding proteins[42] that contribute to lipopolysaccharide response in a TLR4 dependent manner.[42] We have previously suggested that proteins of the S100 family are regulated in retinal vein occlusion[22] and our study indicates that the turnover of S100 proteins is altered in BRVO. However, the S100 proteins did not correlate with CRT and BCVA, and our data does not provide an underlying explanation for the S100 regulation.

Alpha-enolase and contactin-1 were negatively correlated to CRT. BRVO patients with greater than 5 disc diameters of retinal nonperfusion had lower levels of both proteins, indicating that their regulation is related to retinal ischemia. Alpha-enolase is a glycolytic enzyme known to be expressed in the cytoplasm and on cell membranes of retinal ganglion cells, Müller cells, cones, and rods.[43] Changes in retinal alpha-enolase have been observed following experimental retinal detachment,[44] suggesting that the protein is sensitive to retinal stress. Contactin-1 is a cell adhesion protein involved in axonal organization in early central nervous system development.[45] Retinal contactin-1 has been found to be downregulated following hyperglycemia,[46] indicating that contactin-1 is downregulated in retinal stress.

Arterial hypertension is a well-documented risk factor in BRVO.[47] It is a limitation of this study that data on arterial hypertension were not available for patients who donated aqueous samples to the biobank. Although our study achieved good coverage of the aqueous proteome, detection of low abundance proteins remains a challenge in discovery-type proteomics.[11,17] For example, low-abundant proteins, such as VEGF, interleukin-6, and interleukin-8, were not identified in our proteome analysis and VEGF quantification with ELISA was necessary. Detection of low abundance proteins with discovery-type proteomics is limited by a number of factors including sample complexity, technical variation, and fragmentation efficiency. Sample complexity with high dynamic ranges of protein abundances makes detection of low-abundant proteins difficult as protein abundances may stretch over 13 orders of magnitude

Investigative Ophthalmology & Visual Science

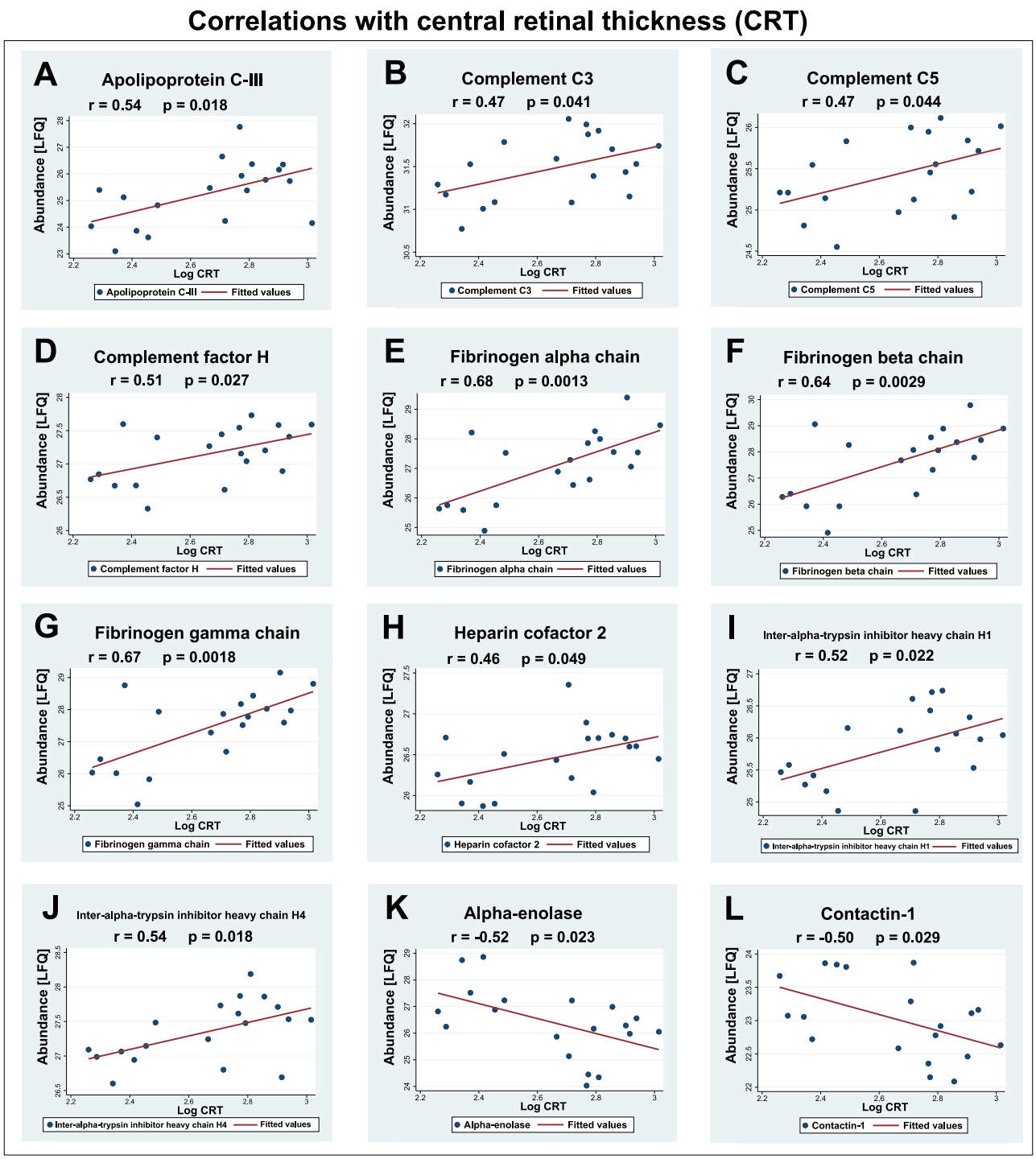

Figure 4. Correlations between aqueous proteins and severity of macular edema measured as central retinal thickness (CRT). CRT values are $\log_{10}$ transformed to obtain normal distribution. LFQ values denote the contents of the proteins measured by mass spectrometry. Correlations are calculated as Pearson's correlation coefficient (r). (**A–J**) Proteins that were significantly positively correlated to severity of macular edema. (**K, L**) Alpha-enolase and contactin-1 were negatively correlated with the severity of macular edema.

depending on the material under study.[48] Low abundance proteins tend to yield larger spectral count variation resulting in underestimation of differences in expression level.[49] Fragmentation efficiency of tryptic peptides remains a limiting factor in identification of lowly abundant proteins.[48] Furthermore, low-abundant proteins with low molecular weight, for example interleukin-8, yield very few tryptic peptides, which makes them complicated to identify with mass spectrometry.[50]

The sample material is another limitation of our study. Key proteins identified with proteomic techniques may correlate with growth factors and cytokines known to be

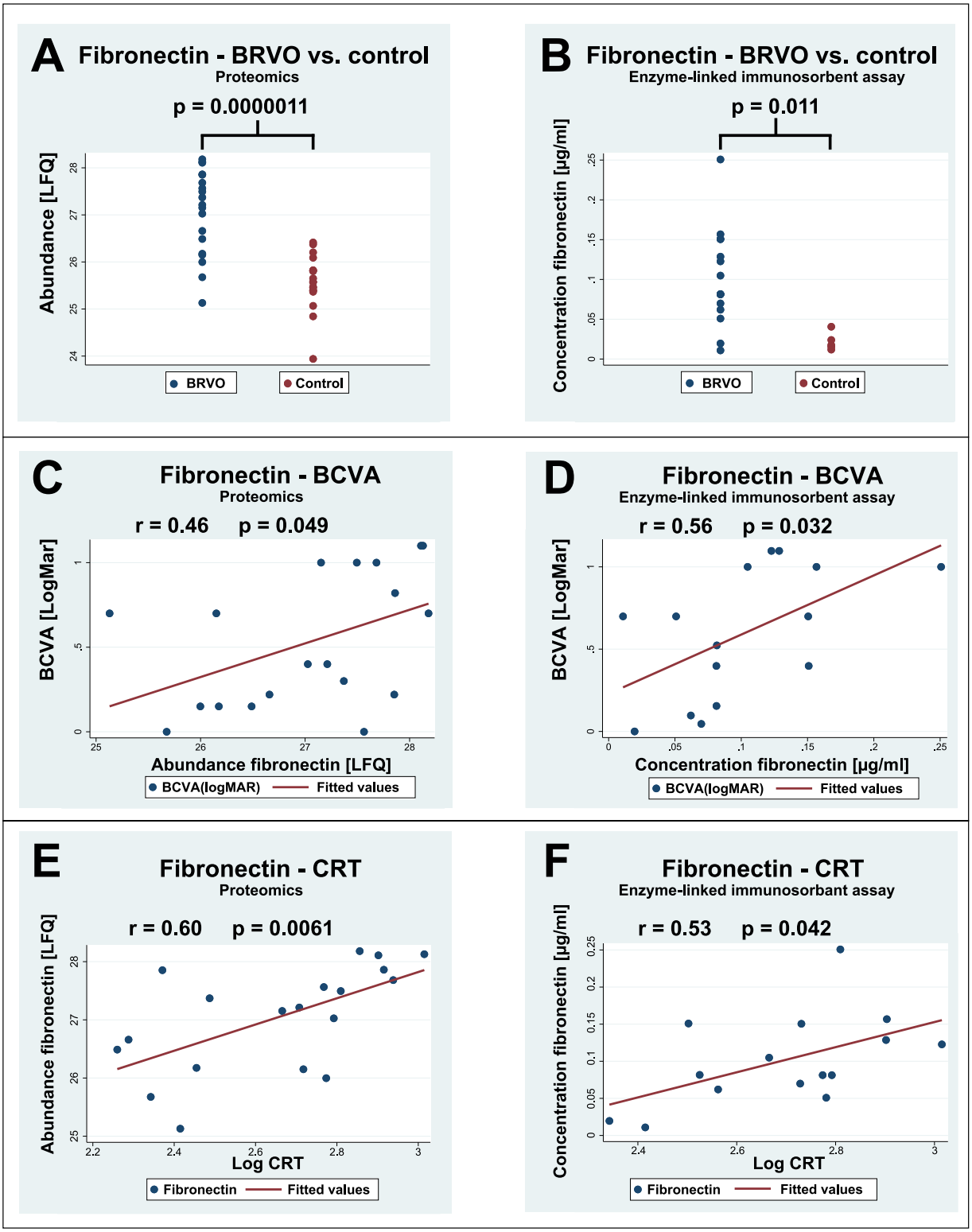

Figure 5. Fibronectin in BRVO. LFQ values denote the content of fibronectin measured in proteomic analysis by mass spectrometry. Correlations are calculated as Pearson's correlation coefficient (*r*). (**A**) Proteomic analysis identified an increased content of fibronectin in BRVO compared with controls. (**B**) The increased content of fibronectin in BRVO was confirmed with ELISA. (**C**) Fibronectin quantified with proteomic analysis correlated with BCVA. (**D**) ELISA analysis confirmed the correlation between fibronectin and BCVA. (**E**) Fibronectin quantified with proteomic analysis correlated with severity of macular edema. (**F**) ELISA analysis confirmed the correlation between fibronectin and severity of macular edema.

Investigative Ophthalmology & Visual Science

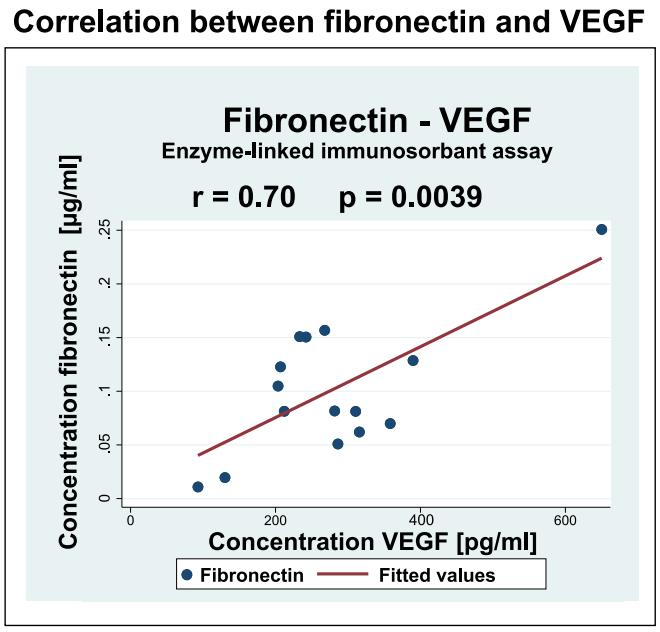

Figure 6. ELISA analysis revealed a significant correlation between fibronectin and VEGF in BRVO.

associated with macular edema in BRVO. For example, the samples could also have been screened for inflammatory proteins, such as interleukin-6 and interleukin-8. Owing to the low volume and the low protein concentration of the aqueous samples, we only had sufficient sample material to verify the correlation between fibronectin and VEGF.

Conclusions

BRVO was associated with multiple aqueous protein changes. Proteome changes were more pronounced in BRVO with greater than 5 disc areas of retinal nonperfusion. Fibronectin was increased in BRVO and higher in BRVO with greater than 5 disc areas of retinal nonperfusion. Fibronectin correlated with BCVA, severity of macular edema and VEGF. Our findings suggest that aqueous fibronectin may reflect severity and vascular permeability in BRVO. Multiple proteins were correlated to the size of macular edema indicating that macular edema is a multifactorial complication. The plasma proteins apolipoprotein C-III, complement C3, complement C5, complement factor H, and fibrinogen chains were increased in BRVO and correlated with severity of macular edema. Alpha-enolase and contactin-1 were negatively correlated with severity of macular edema. Our study indicated that the expression of alpha-enolase and contactin-1 is related to retinal nonperfusion. The proinflammatory proteins LBP, CD14, S100A7, S100A8, and S100A9 were regulated in BRVO and may contribute to an inflammatory response in BRVO.

Table 5. BRVO with Greater Than 5 Disc Areas of Retinal Nonperfusion Versus BRVO with Less Than or Equal to 5 Disc Areas of Retinal Nonperfusion

Protein ID	Protein Name	Gene Name	*P* Value	Fold Change Ischemia/Nonischemia
P02675	Fibrinogen beta chain	FGB	1.86×10^{-5}	5.18
P02679	Fibrinogen gamma chain	FGG	1.60×10^{-5}	4.16
P02656	Apolipoprotein C-III	APOC3	0.00014	4.06
P02671	Fibrinogen alpha chain	FGA	0.0003	3.83
P68871	Hemoglobin subunit beta	HBB	0.0099	3.67
P02751-3	Fibronectin	FN1	0.00013	2.88
P01876	Ig alpha-1 chain C region	IGHA1	0.0023	2.55
P27169	Serum paraoxonase/arylesterase 1	PON1	0.00089	2.12
P06727	Apolipoprotein A-IV	APOA4	0.0037	2.07
P02746	Complement C1q subcomponent subunit B	C1QB	4.13×10^{-5}	1.98
P19827	Inter-alpha-trypsin inhibitor heavy chain H1	ITIH1	0.00017	1.98
P19823	Inter-alpha-trypsin inhibitor heavy chain H2	ITIH2	0.0015	1.84
P02647	Apolipoprotein A-I	APOA1	0.0023	1.71
P08603	Complement factor H	CFH	4.41×10^{-5}	1.65
P01011	Alpha-1-antichymotrypsin	SERPINA3	2.84×10^{-5}	1.59
P02749	Beta-2-glycoprotein 1	APOH	0.0025	1.59
Q96IY4	Carboxypeptidase B2	CPB2	0.00092	1.55
P00747	Plasminogen	PLG	0.0016	1.51
P01024	Complement C3 chain	C3	0.00054	1.50
P05546	Heparin cofactor 2	SERPIND1	0.0012	1.50
P13473	Lysosome-associated membrane glycoprotein 2	LAMP2	0.0011	0.66
P30086	Phosphatidylethanolamine-binding protein 1	PEBP1	0.004	0.64
Q92520	Protein FAM3C	FAM3C	0.0064	0.58
Q12860	Contactin-1	CNTN1	0.0017	0.55
Q15582	Transforming growth factor-beta-induced protein ig-h3	TGFBI	0.0028	0.53
	Neural cell adhesion molecule 1	NCAM1	0.0043	0.53
Q9NQ79	Cartilage acidic protein 1	CRTAC1	5.73×10^{-5}	0.5
P51693	Amyloid-like protein 1	APLP1	0.00051	0.47
Q06481	Amyloid-like protein 2	APLP2	0.0051	0.45
P78509	Reelin	RELN	0.0021	0.37
P06733	Alpha-enolase	ENO1	0.0048	0.29

Investigative Ophthalmology & Visual Science

Acknowledgments

The authors thank Mona Britt Hansen, Aarhus University, Aarhus, Denmark, for her expert technical assistance; and Orthoptist Roy Ewan, Department of Ophthalmology, Odense University Hospital, Odense, Denmark, for assisting the authors with English editing of the manuscript. The authors thank Fight for Sight Denmark, Helene og Viggo Bruuns Fond, the Svend Andersen Foundation, Synoptik-Fonden, the Herta Christensen Foundation, the North Denmark Region (2013-0076797), Speciallæge Heinrich Kopps Legat, and the Danish Ophthalmological Society for their generous support. The mass spectrometers used for the study were funded by A.P. Møller og Hustru Chastine Mc-Kinney Møllers Fond til almene Formaal.

Disclosure: **L.J. Cehofski**, None; **K. Kojima**, None; **N. Terao**, None; **K. Kitazawa**, None; **S. Thineshkumar**, None; **J. Grauslund**, None; **H. Vorum**, None; **B. Honoré**, None

References

1. Rehak J, Rehak M. Branch retinal vein occlusion: pathogenesis, visual prognosis, and treatment modalities. *Curr Eye Res*. 2008;33:111–131.
2. Noma H, Funatsu H, Mimura T. Association of electroretinographic parameters and inflammatory factors in branch retinal vein occlusion with macular oedema. *Br J Ophthalmol*. 2012;96:1489–1493.
3. Noma H, Funatsu H, Mimura T. Vascular endothelial growth factor and interleukin-6 are correlated with serous retinal detachment in central retinal vein occlusion. *Curr Eye Res*. 2012;37:62–67.
4. Noma H, Funatsu H, Mimura T, Eguchi S. Vascular endothelial growth factor receptor-2 in macular oedema with retinal vein occlusion. *Ophthalmic Res*. 2012;48:56–58.
5. Noma H, Funatsu H, Mimura T, Eguchi S, Shimada K. Inflammatory factors in major and macular branch retinal vein occlusion. *Ophthalmologica*. 2012;227:146–152.
6. Noma H, Mimura T. Aqueous soluble vascular endothelial growth factor receptor-2 in macular edema with branch retinal vein occlusion. *Curr Eye Res*. 2013;38:1288–1290.
7. Noma H, Mimura T, Eguchi S. Association of inflammatory factors with macular edema in branch retinal vein occlusion. *JAMA Ophthalmol*. 2013;131:160–165.
8. Noma H, Mimura T, Yasuda K, Shimura M. Role of soluble vascular endothelial growth factor receptor signaling and other factors or cytokines in central retinal vein occlusion with macular edema. *Invest Ophthalmol Vis Sci*. 2015;56:1122–1128.
9. Noma H, Mimura T, Yasuda K, Shimura M. Role of soluble vascular endothelial growth factor receptors-1 and -2, their ligands, and other factors in branch retinal vein occlusion with macular edema. *Invest Ophthalmol Vis Sci*. 2014;55:3878–3885.
10. Noma H, Yasuda K, Shimura M. Cytokines and the pathogenesis of macular edema in branch retinal vein occlusion. *J Ophthalmol*. 2019;2019:5185128.
11. Cehofski LJ, Honore B, Vorum H. A review: proteomics in retinal artery occlusion, retinal vein occlusion, diabetic retinopathy and acquired macular disorders. *Int J Mol Sci*. 2017;18:907.
12. Funke S, Markowitsch S, Schmelter C, et al. In-depth proteomic analysis of the porcine retina by use of a four step differential extraction bottom up LC MS platform. *Mol Neurobiol*. 2017;54:7262–7275.
13. Funke S, Schmelter C, Markowitsch SD, et al. Comparative quantitative analysis of porcine optic nerve head and retina subproteomes. *Int J Mol Sci*. 2019;20:4229.
14. Schmelter C, Fomo KN, Perumal N, et al. Synthetic polyclonal-derived CDR peptides as an innovative strategy in glaucoma therapy. *J Clin Med*. 2019;8:1222.
15. Schmelter C, Funke S, Treml J, et al. Comparison of two solid-phase extraction (SPE) methods for the identification and quantification of porcine retinal protein markers by LC-MS/MS. *Int J Mol Sci*. 2018;19:3847.
16. Schmelter C, Perumal N, Funke S, Bell K, Pfeiffer N, Grus FH. Peptides of the variable IgG domain as potential biomarker candidates in primary open-angle glaucoma (POAG). *Hum Mol Genet*. 2017;26:4451–4464.
17. Cehofski LJ, Mandal N, Honore B, Vorum H. Analytical platforms in vitreoretinal proteomics. *Bioanalysis*. 2014;6:3051–3066.
18. Yao J, Chen Z, Yang Q, et al. Proteomic analysis of aqueous humor from patients with branch retinal vein occlusion-induced macular edema. *Int J Mol Med*. 2013;32:1421–1434.
19. Honore B. Proteomic protocols for differential protein expression analyses. *Methods Mol Biol*. 2020;2110:47–58.
20. Christakopoulos C, Cehofski LJ, Christensen SR, Vorum H, Honore B. Proteomics reveals a set of highly enriched proteins in epiretinal membrane compared with inner limiting membrane. *Exp Eye Res*. 2019;186:107722.
21. Tyanova S, Temu T, Cox J. The MaxQuant computational platform for mass spectrometry-based shotgun proteomics. *Nat Protoc*. 2016;11:2301–2319.
22. Cehofski LJ, Kruse A, Kirkeby S, et al. IL-18 and S100A12 are upregulated in experimental central retinal vein occlusion. *Int J Mol Sci*. 2018;19:3328.
23. Tusher VG, Tibshirani R, Chu G. Significance analysis of microarrays applied to the ionizing radiation response. *Proc Natl Acad Sci U S A*. 2001;98:5116–5121.
24. Tabas-Madrid D, Nogales-Cadenas R, Pascual-Montano A. GeneCodis3: a non-redundant and modular enrichment analysis tool for functional genomics. *Nucleic Acids Res*. 2012;40:W478–W483.
25. Carmona-Saez P, Chagoyen M, Tirado F, Carazo JM, Pascual-Montano A. GENECODIS: a web-based tool for finding significant concurrent annotations in gene lists. *Genome Biol*. 2007;8:R3.
26. Nogales-Cadenas R, Carmona-Saez P, Vazquez M, et al. GeneCodis: interpreting gene lists through enrichment analysis and integration of diverse biological information. *Nucleic Acids Res*. 2009;37:W317–W322.
27. Cehofski LJ, Kruse A, Kjaergaard B, Stensballe A, Honore B, Vorum H. Proteins involved in focal adhesion signaling pathways are differentially regulated in experimental branch retinal vein occlusion. *Exp Eye Res*. 2015;138:87–95.
28. Szklarczyk D, Franceschini A, Wyder S, et al. STRING v10: protein-protein interaction networks, integrated over the tree of life. *Nucleic Acids Res*. 2015;43:D447–D452.
29. Szklarczyk D, Gable AL, Lyon D, et al. STRING v11: protein-protein association networks with increased coverage, supporting functional discovery in genome-wide experimental datasets. *Nucleic Acids Res*. 2019;47:D607–D613.
30. Szklarczyk D, Morris JH, Cook H, et al. The STRING database in 2017: quality-controlled protein-protein association networks, made broadly accessible. *Nucleic Acids Res*. 2017;45:D362–D368.
31. Vesaluoma M, Mertaniemi P, Mannonen S, et al. Cellular and plasma fibronectin in the aqueous humour of primary open-angle glaucoma, exfoliative glaucoma and cataract patients. *Eye (Lond)*. 1998;12(Pt 5):886–890.

32. Kim KS, Lee BH, Kim IS. The measurement of fibronectin concentrations in human aqueous humor. *Korean J Ophthalmol*. 1992;6:1–5.
33. Li X, Gao Y, Li J, et al. FOXP3 inhibits angiogenesis by down-regulating VEGF in breast cancer. *Cell Death Dis*. 2018;9:744.
34. Miller CG, Budoff G, Prenner JL, Schwarzbauer JE. Minireview: fibronectin in retinal disease. *Exp Biol Med (Maywood)*. 2017;242:1–7.
35. Lemanska-Perek A, Adamik B. Fibronectin and its soluble EDA-FN isoform as biomarkers for inflammation and sepsis. *Adv Clin Exp Med*. 2019;28:1561–1567.
36. Faralli JA, Filla MS, Peters DM. Role of fibronectin in primary open angle glaucoma. *Cells*. 2019;8:1518.
37. Wang Y, Reheman A, Spring CM, et al. Plasma fibronectin supports hemostasis and regulates thrombosis. *J Clin Invest*. 2014;124:4281–4293.
38. Miller JW, Le Couter J, Strauss EC, Ferrara N. Vascular endothelial growth factor a in intraocular vascular disease. *Ophthalmology*. 2013;120:106–114.
39. Noma H, Funatsu H, Yamasaki M, et al. Pathogenesis of macular edema with branch retinal vein occlusion and intraocular levels of vascular endothelial growth factor and interleukin-6. *Am J Ophthalmol*. 2005;140:256–261.
40. Zanoni I, Granucci F. Role of CD14 in host protection against infections and in metabolism regulation. *Front Cell Infect Microbiol*. 2013;3:32.
41. Stasi A, Intini A, Divella C, et al. Emerging role of lipopolysaccharide binding protein in sepsis-induced acute kidney injury. *Nephrol Dial Transplant*. 2017;32:24–31.
42. Holzinger D, Foell D, Kessel C. The role of S100 proteins in the pathogenesis and monitoring of autoinflammatory diseases. *Mol Cell Pediatr*. 2018;5:7.
43. Braithwaite T, Vugler A, Tufail A. Autoimmune retinopathy. *Ophthalmologica*. 2012;228:131–142.
44. Mandal N, Lewis GP, Fisher SK, et al. Protein changes in the retina following experimental retinal detachment in rabbits. *Mol Vis*. 2011;17:2634–2648.
45. Chatterjee M, Schild D, Teunissen CE. Contactins in the central nervous system: role in health and disease. *Neural Regen Res*. 2019;14:206–216.
46. Sharma S, Chakravarthy H, Suresh G, Devanathan V. Adult goat retinal neuronal culture: applications in modeling hyperglycemia. *Front Neurosci*. 2019;13:983.
47. Newman-Casey PA, Stem M, Talwar N, Musch DC, Besirli CG, Stein JD. Risk factors associated with developing branch retinal vein occlusion among enrollees in a United States managed care plan. *Ophthalmology*. 2014;121:1939–1948.
48. Harney DJ, Hutchison AT, Su Z, et al. Small-protein enrichment assay enables the rapid, unbiased analysis of over 100 low abundance factors from human plasma. *Mol Cell Proteomics*. 2019;18:1899–1915.
49. Lee HY, Kim EG, Jung HR, et al. Refinements of LC-MS/MS spectral counting statistics improve quantification of low abundance proteins. *Sci Rep*. 2019;9:13653.
50. Geiger T, Cox J, Mann M. Proteomics on an Orbitrap benchtop mass spectrometer using all-ion fragmentation. *Mol Cell Proteomics*. 2010;9:2252–2261.